Macromolecules

Article

pubs.acs.org/Macromolecules

Significant Improved Performance of Photovoltaic Cells Made from a Partially Fluorinated Cyclopentadithiophene/Benzothiadiazole Conjugated Polymer

Yong Zhang, Jingyu Zou, Chu-Chen Cheuh, Hin-Lap Yip, and Alex K.-Y. Jen*

Department of Materials Science and Engineering, University of Washington, Seattle, Washington, 98195, United States

Supporting Information

ABSTRACT: A partially fluorinated low bandgap polymer, poly-[2,6-(4,4-bis(2-ethylhexyl)-4*H*-cyclopenta [2,1-b;3,4-*b*′]-dithiophene)-*alt*-4,7-(5-fluoro-[2,1,3]-benzothiadiazole)] (PCPDTFBT) was synthesized through a microwave-assisted Stille polymerization. It was found that PCPDTFBT has better $\pi-\pi$ stacking in solution than its nonfluorinated analogue, poly[2,6-(4,4-bis(2-ethylhexyl)-4*H*-cyclopenta[2,1-b;3,4-*b*′]dithiophene)-*alt*-4,7-([2,1,3]-benzothiadiazole)] (PCPDTBT), resulting in 2 times higher hole mobility. Power conversion efficiency (PCE) of the device using PCPDTFBT/$PC_{71}BM$ as active layer (5.51%) is much higher than the device using PCPDTBT/$PC_{71}BM$ (2.75%) that was fabricated under the same condition without using any solvent additive to modify the morphology. The significantly enhanced PCE is the result of improved open circuit voltage and short circuit current coming from the lower lying HOMO energy level and the appropriate morphology of PCPDTFBT. In addition, the device with PCPDTFBT/$PC_{71}BM$ could also be processed from nonchlorinated organic solvents such as *o*-xylene to obtain high PCE of 5.32% (which is the highest value for PCPDTBT type polymers processed without using chlorinated solvents). Further device optimization by inserting a thin layer of fullerene-containing surfactant between the active layer and Ag cathode resulted in even higher PCE of 5.81%. These encouraging results showed that PCPDTFBT has the potential to be used as a low bandgap polymer to provide complementary absorption in tandem solar cells.

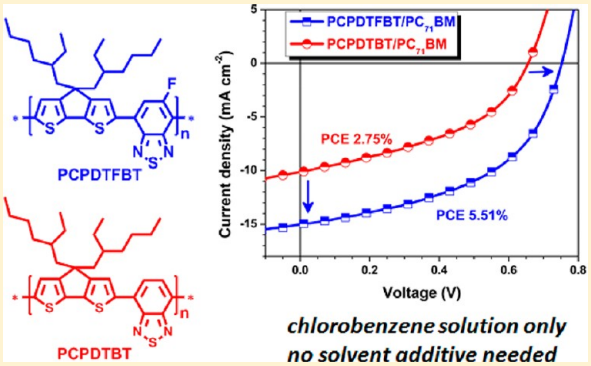

1. INTRODUCTION

Bulk heterojunction (BHJ) based polymer solar cells (PSCs), in which conjugated polymers are blended with fullerene derivatives (i.e., PCBM), are very promising for realizing the goal of achieving low-cost and scalable renewable energy.[1−4] Over the past decade, the power conversion efficiency (PCE) of PSCs has been steadily increased to above 8% through various optimizations of conjugated polymers, material/electrode interfaces, and device architectures.[5−13] One of the most important developments for conjugated polymers is the rational design of narrow band gap polymers to better match the solar spectrum.[1] In general, these polymers are copolymers based on an electron-rich donor (D) and an electron-deficient acceptor (A) on the polymer backbone to facilitate the intramolecular charge transfer between D and A. The molecular units such as carbazole, benzodithiophene, and cyclopentadithiophene, etc., have been used as the donor, and benzothiadiazole, thienothiophene, and thienopyrroledione, etc., have been commonly used as the acceptor.[5,6,14−25]

The morphological control of the BHJ active layer in PSC plays a key role in charge generation, separation and transport within the device.[26,27] The ideal morphology contains a phase separation between polymer donor and fullerene acceptor to form an interpenetrating network of ∼10 nm length. To maximize the photovoltaic performance, various methods, such as thermal annealing, vapor annealing, and solvent additives have been used to control the morphology for achieving optimal phase separation.[28,29] Bazan and Heeger et al. have shown that the morphology of the active blend can be effectively controlled by adding a small amount of high boiling point solvent such as 1,8-dithioloctane (DTO) or 1,8-diiodooctane (DIO) into the polymer solution. For example, the devices made from poly[2,6-(4,4-bis(2-ethylhexyl)-4*H*-cyclopenta[2,1-b;3,4-*b*′]dithiophene)-*alt*-4,7-(2,1,3-benzothiadiazole)] (PCPDTBT) could reach much higher PCE by adding a small amount of DTO or DIO into the PCPDTBT/$PC_{71}BM$ solution in chlorobenzene.[28,30] The optimized PCPDTBT/$PC_{71}BM$ devices showed a J_{sc} of ∼15−16 mA cm^{-2}, a V_{oc} of 0.37−0.6 V, a fill factor (FF) of 40−55%, and a PCE of between 3.5 to 5.4%.[28,30,31] However, without solvent additive, the PCPDTBT/PCBM-based devices only gave a PCE of 2.6−3.2% and a low J_{sc} of 8−11 mA cm^{-2} because of the formation of unfavorable morphology.[28,32] Another well-studied polymer, poly[(4,4′-bis(2-ethylhexyl)dithieno[3,2-

Received: May 6, 2012
Revised: June 12, 2012
Published: June 22, 2012

   dx.doi.org/10.1021/ma3009178 | *Macromolecules* 2012, 45, 5427−5435

Scheme 1. Synthesis of Monomers and Polymer

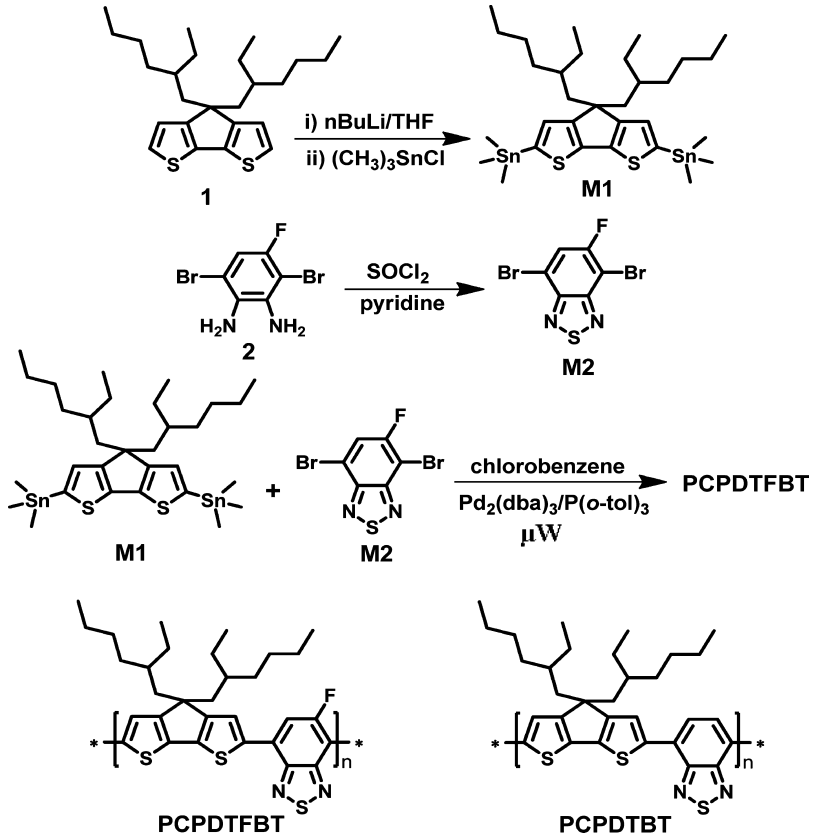

b:2′,3′-d]silole)-2,6-diyl-*alt*-((5-octylthieno[3,4-c]pyrrole-4,6-dione)-1,3-diyl)] (PDTSTPD), also showed significant morphological changes upon the addition of processing additive. Without DIO in processing solvent, the device performance of PDTSTPD only showed a PCE of less than 1%. After adding 2% DIO, the PCE of PDTSTPD device dramatically increased to ~7% due to the improved morphology.[33] These results showed that proper control of the morphology is very critical to improve the overall performance of device. However, these small amounts (0.2−3%) of high boiling point solvent additives are difficult to control and remove afterward. In addition, the tedious processing conditions are also unfavorable for large-area inkjet or roll-to-roll printing due to possible residual solvent in the device.[34,35] Therefore, it would be ideal if a conjugated polymer/PCBM blend can be processed from single solvent system to afford optimal morphology for fabricating high-performance PSC.[34,35]

Recently, the introduction of fluorine (F) atom onto conjugated polymer backbone has been proven to be an effective way to enhance the overall performance of PSCs.[7,8,36] The F atom plays two important roles: (1) the electron-withdrawing property of F atom can lower the highest occupied molecular orbital (HOMO) energy level, therefore, results in an increased V_{oc} in the corresponding device; (2) F atom can form F−H, F−F bonding through inter- or intramolecular interactions, which may affect $\pi-\pi$ stacking of polymer to fine-tune its morphology with fullerene.

Herein, we report a fluorinated polymer, PCPDTFBT (Scheme 1), synthesized via Stille polymerization of mono-fluoro-substituted benzothiadiazole and distannylcyclopentadithiophene. Better $\pi-\pi$ stacking in PCPDTFBT enables PCPDTFBT/$PC_{71}BM$ blend based PSC to have a promising PCE of 5.51% with higher V_{oc} (0.75 V) compared to its PCPDTBT/$PC_{71}BM$ analogue (<0.6 V). Most importantly, this performance was achieved without using any solvent additive. We have also demonstrated that PCPDTFBT can be processed from a nonchlorinated solvent, *o*-xylene to achieve a high PCE of 5.32%, which is the best performance reported so far for devices processed from nonchlorinated solvents. Furthermore, an even higher PCE of 5.81% could also be achieved after inserting a thin layer of fullerene-containing surfactant between the active layer and Ag cathode to facilitate the extraction of electrons.

2. RESULTS AND DISCUSSIONS

2.1. Synthesis. Scheme 1 shows the synthetic route of PCPDTFBT. Compounds **1** and **M1** were synthesized from literature reported methods.[32] The synthesis of **M2** involves a multistep synthesis starting from 2,5-dibromo-3-fluorobenzene as shown in our previous paper.[36] It is difficult to achieve high molecular weight polymer under conventional oil-bath heating because the **M1** monomer is difficult to purify by column chromatography or recrystallization.[31] Hence, PCPDTFBT was synthesized through a microwave-assisted Stille polymerization, which has been demonstrated to be effective in increasing the molecular weight.[31] Purifications were performed by reprecipitation and Soxhlet extraction of the crude polymers with acetone and hexane to remove oligomers and residual catalyst. Because of the asymmetrical FBT monomer, it is worthy to note that PCPDTFBT is a regiorandom polymer. The number-average molecular weight (M_n) of PCPDTFBT was determined to be 23.4 kDa with a PDI of 1.54. PCPDTBT was prepared also under the same condition with a M_n of 21.3 kDa and a PDI of 1.78. The solubility of PCPDTFBT is strongly varied with

dx.doi.org/10.1021/ma3009178 | *Macromolecules* 2012, 45, 5427−5435

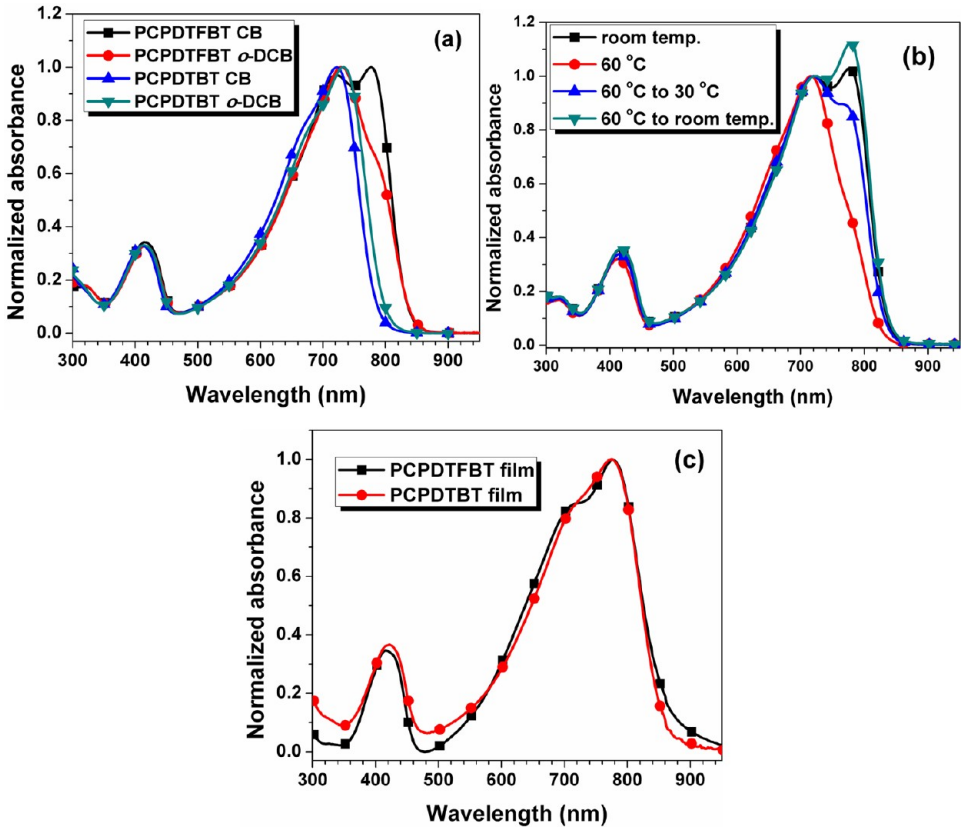

Figure 1. The UV–vis spectra of PCPDTFBT and PCPDTBT in CB and *o*-DCB solutions (a), PCPDTFBT in CB solution under different temperatures (b) and in thin films (c) of both polymers.

different solvents. It was found that PCPDTFBT possesses good solubility in *o*-dichlorobenzene (DCB), CB and *o*-xylene, but has limited solubility in chloroform. However, PCPDTBT is soluble in all above-mentioned solvents although they have similar molecular weights, which indicates that PCPDTFBT has stronger packing in solution than PCPDTBT.

2.2. Optical Properties. The UV–vis absorption spectra of PCPDTFBT and PCPDTBT were investigated in both CB and DCB solutions and in thin film (Figure 1). As shown in Figure 1a, PCPDTBT in CB and DCB solutions showed a characteristic peak at the low energy absorption band, which is attributed to the intramolecular charge transfer (ICT) band between CPDT and BT.[16,32] A slightly red-shifted ICT peak (732 nm) was found in DCB solution compared to that was observed in CB solution (722 nm). This could be due to the better solubility of PCPDTBT in DCB than in CB solution. However, it is interesting to find a double peak at the low energy absorption band for PCPDTFBT in CB solution (Figure 1a). The peak at 722 nm is similar to that of PCPDTBT; however, the stronger intensity peak at 776 nm is believed to be the result of $\pi-\pi$ stacking of PCPDTFBT polymer chains. In DCB solution, PCPDTFBT still showed a certain degree of packing which is evident by the shoulder peak at ~770 nm compared to the main ICT peak at 730 nm (Figure 1a). The absorption onsets of PCPDTFBT in both CB and DCB solutions are almost the same at 850 nm. The lower intensity of the $\pi-\pi$ stacking peak in DCB compared to that in CB is attributed to the better solubility of polymer in DCB than in CB.

To further verify the packing behavior, the CB solution of PCPDTFBT was heated to 60 °C to measure its UV–vis spectrum. As shown in Figure 1b, the packing peak at 776 nm is almost disappeared due to the breakup of polymer $\pi-\pi$ stacking (aggregation) upon heating. When the solution was cooled to ~30 °C, however, an intense packing peak reappeared (Figure 1b). Further cooling of the solution to room temperature ("cold" solution), the packing induced peak became even more evident. In "warm" solution, the thermal history was removed and the PCPDTFBT chains were fully dissolved and freely extended and rotated compared to those in "cold" solution. Under slow cooling, these polymer chains aggregate due to stronger intermolecular interaction, therefore, a stronger stacking peak was observed in the "cold" solution.

However, the absorption of PCPDTBT did not show such changes, only blue-shifted during the temperature cycles.[31] These results clearly showed that PCPDTFBT has stronger stacking than PCPDTBT due to subtle F–H and/or F–F interactions.[7] Figure 1c showed the absorption spectra of PCPDTFBT and PCPDTBT in thin films. Both polymers possess almost the same peaks and onset due to similar polymer backbone. The introduction of F atom onto BT unit seems to have little effect on the absorption spectra, regardless the polymer stacking.[36] The absorption maxima for PCPDTFBT and PCPDTBT are at 776 nm, which is similar to the stacking peak observed for PCPDTFBT in CB solution. The onset of thin film absorption for both polymers is 860 nm, which corresponds to an optical bandgap of 1.44 eV.[28]

2.3. Electrochemical Properties. The CV curves of PCPDTFBT and PCPDTBT in thin films are shown in Figure 2. The HOMO energy level was determined from the onset of oxidative peak. The LUMO energy level was calculated from the difference between the HOMO energy level and the optical

dx.doi.org/10.1021/ma3009178 | *Macromolecules* 2012, 45, 5427–5435

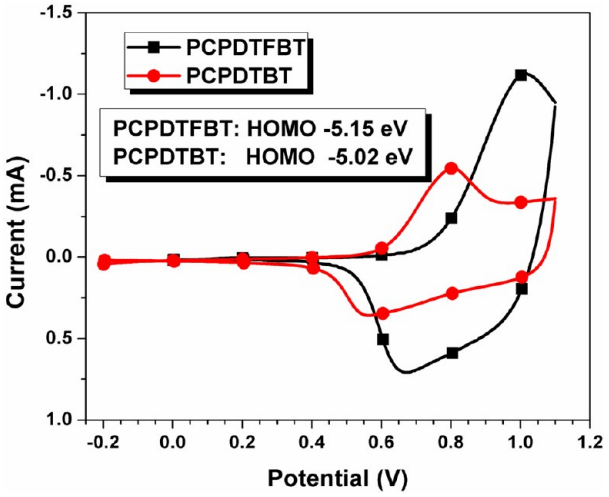

Figure 2. CV curves of PCPDTFBT and PCPDTBT films.

bandgap. As shown in Figure 2, PCPDTFBT and PCPDTBT showed similar oxidative behavior with good reversible peaks. The HOMO of PCPDTFBT was determined to be −5.15 eV compared to −5.02 eV for PCPDTBT, which is similar to the value reported in literature.[28,30] A deeper HOMO energy level (0.13 eV) was found for PCPDTFBT compared to that of PCPDTBT after introducing a F atom onto the BT unit. Therefore, a higher V_{oc} in PCPDTFBT-based PSCs can be expected due to deeper HOMO level of PCPDTFBT than PCPDTBT. The LUMO levels of PCPDTFBT and PCPDTBT are calculated to be −3.71 eV and −3.58 eV, respectively. The reasonably large difference (>0.4 eV) between the LUMO levels of polymer and PCBM should enable efficient charge separation in PSC.

2.4. Charge Transporting Properties of Polymers. The mobility of polymer is one of the key parameters for achieving efficient polymer solar cell performance.[37−39] The polymer field-effect transistors (FETs) were fabricated with top-contact and bottom-gate geometry. SiO_2 was used as the gate dielectric with divinyltetramethyldisiloxane-bis(benzocyclobutene) (BCB) as the buffer layer. Detailed fabrication procedures can be found in the Experimental Section. Figure 3 shows the output and transfer characteristics of PCPDTFBT for positive and negative. It is interesting to note that both polymers showed ambipolar behavior, which may be beneficial for the performance of solar cells. The charge carrier mobilities (μ) of both devices were extracted from the following equation:

$$I_{ds} = \frac{1}{2}\frac{W}{L}\mu C_i(V_G - V_T)^2$$

Here W is the channel width, L is the channel length, C_i is the gate dielectric capacitance per unit area, and V_G is the gate voltage. The hole mobility of the PCPDTFBT and PCPDTBT devices in the saturated region are 1.4×10^{-2} cm^2 V^{-1} S^{-1} and 6.8×10^{-3} cm^2 V^{-1} S^{-1}, respectively.

Since there is only a small variation of the polymer backbone, the enhanced hole mobility of PCPDTFBT should be the result of stronger $\pi-\pi$ stacking which facilitates charge transport. The electron mobility of PCPDTFBT and PCPDTBT are 1.2×10^{-3} cm^2 V^{-1} S^{-1} and 1.8×10^{-3} cm^2 V^{-1} S^{-1}, respectively which are almost at the same order with hole mobility. These combined ambioplar property and higher hole mobility of

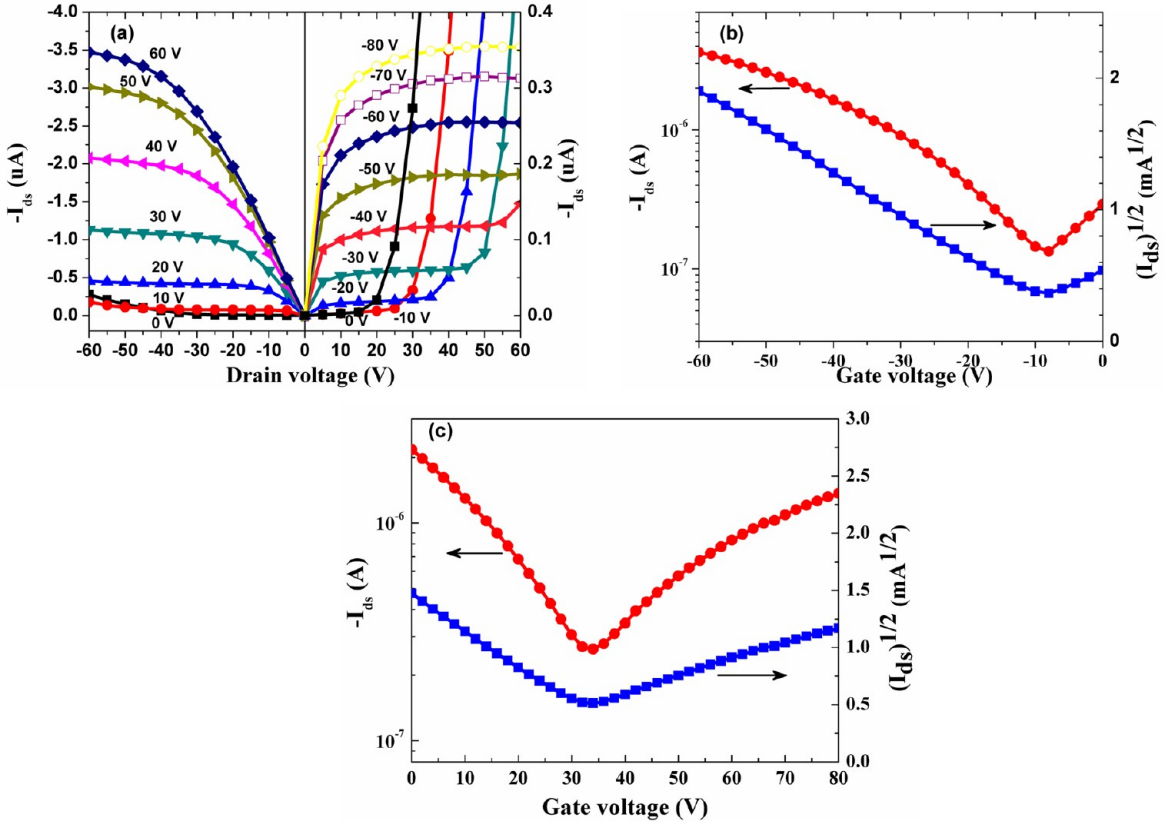

Figure 3. Typical output characteristics (a) and the typical transfer characteristics (b, c) of PCPDTFBT.

dx.doi.org/10.1021/ma3009178 | Macromolecules 2012, 45, 5427−5435

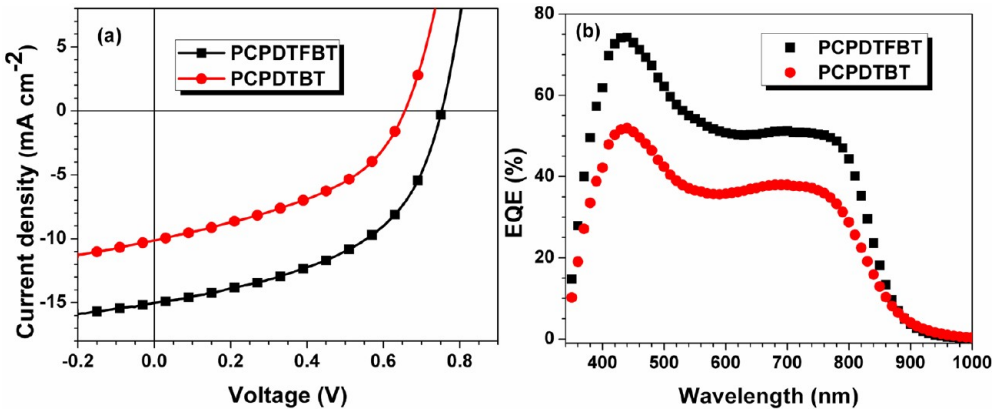

Figure 4. $J-V$ (a) and EQE (b) curves of PCPDTFBT and PCPDTBT devices processed from chlorobenzene solutions.

PCPDTFBT are beneficial to the photovoltaic performance, especially to current density and fill factor.

2.5. Bulk Heterojunction Photovoltaic Device Performance. *2.5.1. Performance of Devices Processed from Chlorobenzene Solutions.* The photovoltaic devices of PCPDTFBT were investigated in the configuration of ITO/PEDOT:PSS/polymer:$PC_{71}BM$/Ca/Al. PCPDTBT-based devices were also made under the same condition for direct comparison. Detailed fabrication and characterization are shown in the Experimental Section. The $J-V$ curves of PCPDTFBT/$PC_{71}BM$ and PCPDTBT/$PC_{71}BM$ devices are shown in Figure 4a. The optimized polymer to $PC_{71}BM$ ratio is 1:2. The active layers were processed from their pure CB solutions without any additive. The device performance is shown in Table 1. The PCPDTFBT/$PC_{71}BM$ device showed a promising PCE of 5.51% with a V_{oc} of 0.75 V, a J_{sc} of 15.0 mA cm^{-2}, and a FF of 49%. However, the PCPDTBT/$PC_{71}BM$ device only gave lower values with a V_{oc} of 0.65 V, a J_{sc} of 10.1 mA cm^{-2}, and a FF of 42% which results in a PCE of 2.75%. The theoretical V_{oc} is calculated to be 0.75 and 0.62 V under the equation of $V_{oc} = 1/e(|E^{donor}_{HOMO}| - |E^{PCMB}_{LUMO}|) - 0.3$ V considering the LUMO level of PCBM to be −4.10 eV.[16,40]

Table 1. Device Performance of PCPDTFBT and PCPDTBT Devices

active layer (solvent)	cathode	V_{oc} (V)	J_{sc} (mA cm^{-2})	FF (%)	PCE (%)
PCPDTBT/$PC_{71}BM$ (CB)[a]	Ca/Al	0.65	10.1	42	2.75
PCPDTFBT/$PC_{71}BM$ (CB)[b]	Ca/Al	0.75	15.0	49	5.51
PCPDTFBT/$PC_{71}BM$ (*o*-xylene)[c]	Ca/Al	0.77	14.4	48	5.32
PCPDTFBT/$PC_{71}BM$ (CB)[b]	Bis-C60/Ag	0.76	15.0	51	5.81

[a]~95 nm. [b]~120 nm. [c]~110 nm.

The external quantum efficiency (EQE) curves of devices are shown in Figure 4b. It can be seen that the devices showed broad response over the range 350−900 nm. The EQE value between 400 to 800 nm for PCPDTFBT devices is more than 50% compared to ~35% for PCPDTBT devices, which is consistent with the result of measured J_{sc}. The integrated J_{sc} from EQE is 10.4 and 14.8 mA cm^{-2}, respectively for PCPDTBT and PCPDTFBT devices, showing the accuracy of measurements. The significantly improved performance in PCPDTFBT/$PC_{71}BM$ device is mainly attributed to higher V_{oc} and J_{sc}.

It is known that the V_{oc} of PSC is proportional to the difference between the HOMO level of polymer and the LUMO level of $PC_{71}BM$, regardless of the cathode modifications. Therefore, the lower lying HOMO level (−5.15 eV) of PCPDTFBT compared to PCPDTBT (−5.02 eV) contributes to the increased V_{oc}. In general, the J_{sc} of a PSC is relevant to the charge mobility and morphology of a BHJ blend. Higher hole mobility measured in PCPDTFBT should also contribute to the higher J_{sc} and FF observed in PCPDTFBT/$PC_{71}BM$ device. It is well-known that proper control of nanoscale morphology of the active layer is also very crucial to the performance of PSCs. Too large or too small phase separation (domains) is not favorable for efficient charge separation, which may lead to severe charge recombination. Figure 5 and 6 showed the TEM and AFM images of the thin film blends of PCPDTBT and PCPDTFBT with $PC_{71}BM$, which were prepared from their CB solutions. As shown in Figure 5, amorphous film was found in PCPDTBT blend film, which is similar to that observed previously.[28,30] The smaller size of phase separation in PCPDTBT blend film increased the possibility for charge recombination, therefore, resulted in lower J_{sc} and FF.[18] Under the same condition, the larger phase separation was observed in PCPDTFBT blend film leading to more efficient charge separation and transport than that of PCPDTBT blend. The AFM images in Figure 6 further provide the evidence for larger phase separation in PCPDTFBT/$PC_{71}BM$ compared to that of PCPDTBT/$PC_{71}BM$. In the PCPDTBT/$PC_{71}BM$ case, it showed a smaller rms of 0.504 nm compared to 1.205 nm for PCPDTFBT/$PC_{71}BM$, which may increase the possibility for charge recombination.

As a result, higher J_{sc} and FF values were obtained in the PCPDTFBT-based device. By combining higher V_{oc}, J_{sc}, and FF, a higher PCE (5.51%) could be reached in PCPDTFBT-based device compared to 2.75% for the PCPDTBT-based device. It is worthy to note that these values were obtained from the pure CB solution of PCPDTFBT/$PC_{71}BM$, without adding any additive. The attempt to add 2−3% of DIO did not further increase the performance of the device. However, the PCPDTBT device with 2% DIO showed an increased PCE (3.69%) with similar J_{sc} but lower V_{oc} (0.59 V).

2.5.2. Performance of Device Processed from o-Xylene Solution. As discussed above, processing solvent is a critical parameter in determining the performance of polymer solar cells.[41−43] In literature, most of the efficient BHJ solar cells

dx.doi.org/10.1021/ma3009178 | *Macromolecules* 2012, 45, 5427−5435

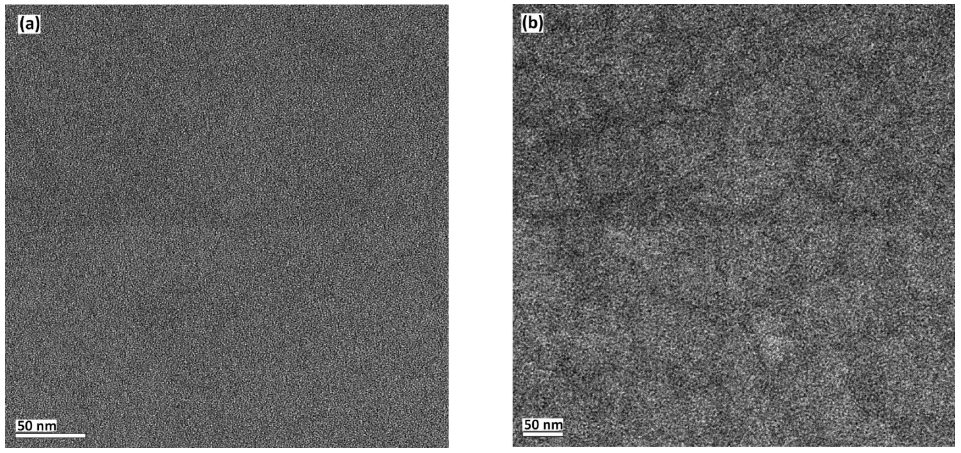

Figure 5. TEM images of PCPDTBT/$PC_{71}BM$ and PCPDTFBT/$PC_{71}BM$ films processed from chlorobenzene solutions.

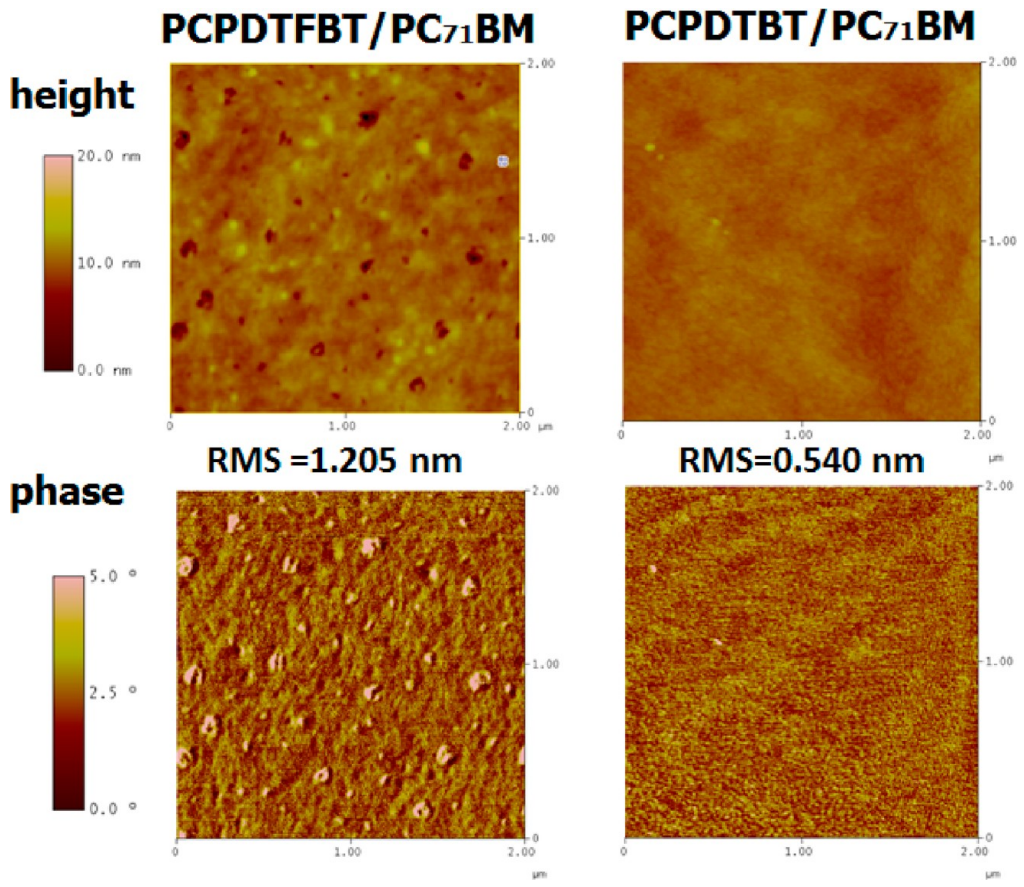

Figure 6. Tapping mode AFM images of PCPDTFBT/$PC_{71}BM$ and PCPDTBT/$PC_{71}BM$ films processed from chlorobenzene solutions.

were processed using chlorinated solvents, such as *o*-DCB and CB, to afford better morphology due to better solubility and viscosity compared to other solvents.[9,20,28,29,38,39] However, chlorinated solvents are not suitable for large scale production due to their high cost, toxicity, and environmental issues. Therefore, it is highly desirable to find an alternative solvent that can be used to afford appropriate morphology during thin film processing to lead to highly efficient PSCs. *o*-Xylene is a good choice because of the similar boiling point and viscosity compared to CB. The most studied polymer using *o*-xylene as solvent is P3HT because of its good solubility.[44−46]

There is very little information about D/A polymer based device that can be processed from *o*-xylene solution to show good efficiency. Since PCPDTFBT has good solubility in *o*-xylene, the active layer of its photovoltaic device can also be processed from its *o*-xylene solution. Figure 7a shows the $J-V$ curve of PCPDTFBT/$PC_{71}BM$ device processed from *o*-xylene solution. The device showed a V_{oc} of 0.77 V, a J_{sc} of 14.4 mA cm^{-2}, and a FF of 48%, which results in an overall PCE of 5.32% (Table 1). This is comparable to device processed from CB solution. To our knowledge, it is one of the highest values reported in literature for device processed from nonchlorinated solvents. This performance is attributed to the appropriate

dx.doi.org/10.1021/ma3009178 | *Macromolecules* 2012, 45, 5427−5435

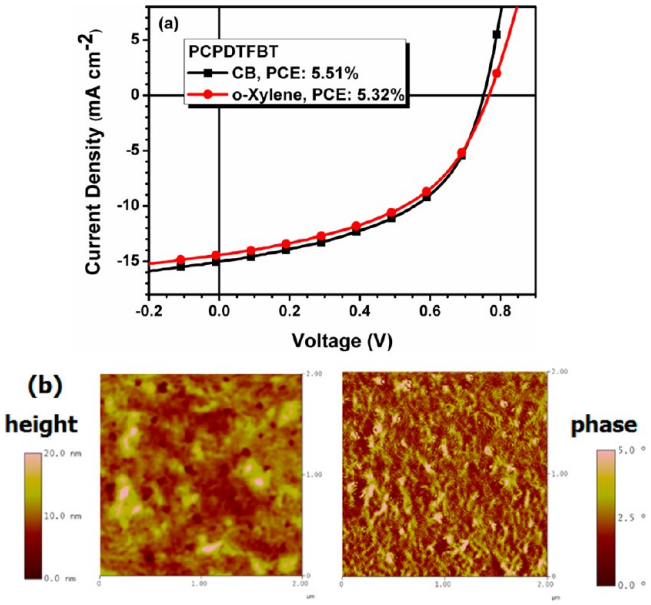

Figure 7. (a) $J-V$ curves of PCPDTFBT/$PC_{71}BM$ devices processed from chlorobenzene and *o*-xylene solutions. (b) AFM images of PCPDTFBT/$PC_{71}BM$ films processed from *o*-xylene solution.

morphology achieved for the blend (Figure 7b). The PCPDTFBT/$PC_{71}BM$ film processed from *o*-xylene solution showed the similar phase separation as the film processed from CB solution (Figure 6).

2.5.3. Device Performance with Hybrid Electron-Collecting Layer/Ag Cathode. Cathode modification for organic electronics has received much attention because the interface between active layer and electrode is critical for achieving optimal device performance.[10,47−52] Water-/alcohol-soluble polymers or polyelectrolytes have been employed as effective interfacial modification materials for improving the performance of PSCs.[48,49,51,53] Recently, we have reported a new alcohol-soluble, bis-adduct fullerene surfactant and its function as an efficient electron selective material when inserted as a thin layer between the active material and high work function cathode, such as Al or Ag.[54] We have adapted this approach here to improve the performance of PCPDTFBT-based devices. The device were fabricated with the configuration of ITO/PEDOT:PSS/PCPDTFBT:$PC_{71}BM$/Bis-C_{60}/Ag. The Bis-C_{60} was spin-coated from its methanol solution. Ag was selected as cathode because it is air stability and good reflectivity. Figure 8 shows the J-V curve of PCPDTFBT/$PC_{71}BM$ device with Bis-C_{60} surfactant as the electron-collecting layer. The PCE was further improved to be 5.81% (a V_{oc} of 0.76 V, a J_{sc} of 15.0 mA cm^{-2}, and a FF of 51%, Table 1), which is even higher than the device with Ca/Al as cathode. This enhancement may be attributed to the efficient charge collection and as an optical buffer between active layer and cathode.[54,55]

3. CONCLUSION

We have designed and synthesized a partially fluorinated low bandgap polymer, PCPDTFBT, through microwave-assisted Stille polymerization between CPDT and FBT units. By introducing F atom onto the BT unit, PCPDTFBT exhibited better $\pi-\pi$ stacking in solution than PCPDTBT. The PSC processed from the solution of PCPDTFBT/$PC_{71}BM$ in CB showed a high PCE of 5.51% compared to 2.75% for

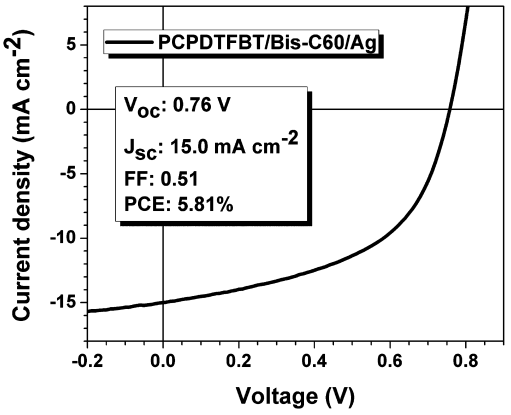

Figure 8. $J-V$ curve of PCPDTFBT-based device with Bis-C_{60} surfactant as an electron-collecting layer and Ag as cathode.

PCPDTBT/$PC_{71}BM$ based device that was fabricated under the same condition. The increased V_{oc} is believed to be the result of lower lying HOMO in PCPDTFBT. The larger phase separation on the order of excition diffusion length and the balanced ambipolar charge mobility contributed to the enhanced J_{sc}. These results showed that the introduction of F atom provides an effective way to simultaneously improve V_{oc} and morphology. Most importantly, there is no need to add any solvent additive to control the morphology of active layer.

Furthermore, PCPDTFBT could also be processed from *o*-xylene and its PSC showed a PCE of 5.32%, which is among the best performance for donor−acceptor type polymers processed from nonchlorinated solvents. In addition, the PCE of PCPDTFBT device could also be increased to reach 5.81% by inserting a thin layer of fullerene-containing surfactant between the active layer and Ag cathode. These encouraging results showed that PCPDTFBT has the potential to be used as a low bandgap polymer to provide complementary absorption in tandem solar cells.

4. EXPERIMENTAL SECTION

General Characterization Methods. UV−vis spectra were measured using a Perkin-Elmer Lambda-9 spectrophotometer. The ^1H NMR spectra were collected on a Bruker AV 500 spectrameter operating at 500 MHz in deuterated chloroform solution with TMS as reference. Cyclic voltammetry of polymer film was conducted in acetonitrile with 0.1 M of tetrabutylammonium hexafluorophosphate using a scan rate of 100 mV s^{-1}. ITO, Ag/AgCl, and Pt mesh were used as working electrode, reference electrode and counter electrode, respectively.

Device Fabrication. Polymer FETs were fabricated through the top-contact and bottom-gate geometry. A thermally grown 300 nm thickness of SiO_2 was purchased from Montco Silicon Technologies INC and used as the gate dielectric. The source/drain regions were defined by a 50 nm thickness of Au through a shadow mask, and the channel length (L) and width (W) was 30 and 1000 μm, respectively. Before gilding the devices, the oxide layer was passivated with a thin divinyltetramethyldisiloxane−bis(benzocyclobutene) (BCB) buffer layer. BCB precursor solution in toluene was spun onto the silicon oxide and subsequently annealed at 250 °C overnight. The total capacitance density measured from parallel-plate capacitors was 10.6 nF/cm^2. Polymer solution in CB was first filtered through 0.2 μm syringe filters, spin-coated onto the BCB-modified substrate, and then annealed at 110 °C for 10 min under nitrogen. Output and transfer characteristics of the transistor devices were performed in a N_2-filled glovebox using an Agilent 4155B semiconductor parameter S6 analyzer. The field-effect mobility was calculated in the saturation regime from the linear fit of $(I_{ds})^{1/2}$ vs V_{gs}. The threshold voltage (V_t)

dx.doi.org/10.1021/ma3009178 | *Macromolecules* 2012, 45, 5427−5435

was estimated as the x intercept of the linear section of the plot of $(I_{ds})^{1/2}$ vs V_{gs}.

PSCs were fabricated using ITO-coated glass substrates (15 Ω/sq), which were cleaned with detergent, deionized water, acetone, and isopropyl alcohol. A thin layer (ca. 30 nm) of PEDOT:PSS (Baytron P VP AI 4083, filtered at 0.45 μm) was first spin-coated on the precleaned ITO-coated glass substrates at 5,000 rpm and baked at 140 °C for 10 min under ambient conditions. The substrates were then transferred into a nitrogen-filled glovebox. Subsequently, the polymer:$PC_{71}BM$ active layer was spin-coated onto the PEDOT:PSS layer. For devices, the solution was prepared by dissolving the polymer and fullerene at a 1:2 weight ratio in chlorobenzene or in o-xylene overnight and filtered through a 0.2 μm PTFE filter, and the substrates were annealed at 110 °C for 10 min prior to electrode deposition. For the device with surfactant, the Bis-C_{60} surfactant in methanol was spin-coated onto the active layer. At the final stage, the substrates were pumped under high vacuum (<2×10^{-6} Torr), and calcium (20 nm) topped with aluminum (100 nm) or silver (100 nm) was thermally evaporated onto the active layer. Shadow masks were used to define the active area (10.08×10^{-2} cm^2) of the devices.

Device Characterization. The current−voltage ($J-V$) characteristics of unencapsulated photovoltaic devices were measured under ambient using a Keithley 2400 source-measurement unit. An Oriel xenon lamp (450 W) with an AM1.5 G filter was used as the solar simulator. A Hamamatsu silicon solar cell with a KG5 color filter, which is traced to the National Renewable Energy Laboratory (NREL), was used as the reference cell. To calibrate the light intensity of the solar simulator, the power of the xenon lamp was adjusted to make the short-circuit current (ISC) of the reference cell under simulated sun light as high as it was under the calibration condition. The spectral mismatches resulting from the test cells, the reference cell, the solar simulator, and the AM1.5 were calibrated with mismatch factors (M). According to Shrotriya et al. the mismatch factor is defined as

$$M = \frac{\int_{\lambda_1}^{\lambda_2} E_{\mathrm{Ref}}(\lambda) S_R(\lambda)\, \mathrm{d}\lambda \int_{\lambda_1}^{\lambda_2} E_S(\lambda) S_T(\lambda)\, \mathrm{d}\lambda}{\int_{\lambda_1}^{\lambda_2} E_{\mathrm{Ref}}(\lambda) S_T(\lambda)\, \mathrm{d}\lambda \int_{\lambda_1}^{\lambda_2} E_S(\lambda) S_R(\lambda)\, \mathrm{d}\lambda}$$

where $E_{ref}(\lambda)$ is the reference spectral irradiance (AM1.5), $E_S(\lambda)$ is the source spectral irradiance, $S_R(\lambda)$ is the spectral responsivity of the reference cell, and $S_T(\lambda)$ is the spectral responsivity of the test cell, each as a function of wavelength (λ). The spectral responsivities of the test cells and the reference cell were calculated from the corresponding external quantum efficiencies (EQE) by the relationship

$$S(\lambda) = \frac{q\lambda}{hc} EQE(\lambda)$$

where the constant term q/hc equals 8.07×10^5 for wavelength in units of meters and $S(\lambda)$ in units of AW^{-1}. The Hamamatsu solar cell was also used as the detector for determining the spectral irradiance of the solar simulator. To minimize the spectral transformation, the irradiance spectrum has been calibrated with the spectral responsively of the Hamamatsu cell and the grating efficiency curve of the monochromator (Oriel Cornerstone 130).

Materials Synthesis. All chemicals, unless otherwise specified, were purchased from Aldrich and used as received. The monomer FBT was synthesized by following the literature method as shown in Scheme S1.[36] Compound **1** was prepared as reported previously.[32] The polymer PCPDTBT was synthesized from compound **1** and 4,7-dibromobenzothiadiazole by following the literature method.[31,32]

Synthesis of PCPDTFBT. In a 10 mL tube, compound 1 (320 mg, 0.44 mmol), FBT (125 mg, 0.40 mmol), $Pd_2(dba)_3$ (7 mg) and P(o-tol)$_3$ (18 mg) were added consequently. After purging for three times with nitrogen, chlorobenzene (3 mL) was added into the mixture. Then, the tube was heated up to 140 °C for 1 h under microwave heating. After cooling to room temperature, the resulted mixture was poured into hexane and stirred for 1 h. The collected precipitate was then dissolved into a small amount of chlorobenzene, which was poured into hexane, and the process was repeated one more time. After filtering, the purple solid was collected and dried overnight under vacuum (140 mg). ^{1}H NMR (o-DCB (o-$C_6D_4Cl_2$), ppm): 8.55−8.35 (d, br, 2H), 7.66 (br, 1H), 2.23 (br, 2H), 1.40−1.18 (d, br, 32H). Molecular weight: M_n = 23.4 kDa, PDI = 1.54.

■ ASSOCIATED CONTENT

Ⓢ Supporting Information

^{1}H NMR spectra of PCPDTFBT. This material is available free of charge via the Internet at http://pubs.acs.org.

■ AUTHOR INFORMATION

Corresponding Author

*E-mail: ajen@u.washington.edu.

Notes

The authors declare no competing financial interest.

■ ACKNOWLEDGMENTS

The authors thank the support from NSF (DMR-0120967), DOE (DEFC3608GO18024/A000), AFOSR (FA9550-09-1-0426), ONR (N00014-11-1-0300), AOARD (FA2386-11-1-4072). C.-C.C. thanks the National Science Council, Taiwan (NSC98-2917-I-564-031) for support. The authors thank Mr. Xi Yang for helping with the TEM measurement.

■ REFERENCES

(1) Chen, J. W.; Cao, Y. *Acc. Chem. Res.* **2009**, *42*, 1709−1718.
(2) Cheng, Y. J.; Yang, S. H.; Hsu, C. S. *Chem. Rev.* **2009**, *109*, 5868−5923.
(3) Krebs, F. C. *Sol. Energy Mater. Sol. Cells* **2009**, *93*, 394−412.
(4) Thompson, B. C.; Frechet, J. M. J. *Angew. Chem., Int. Ed.* **2008**, *47*, 58−77.
(5) Chen, H. Y.; Hou, J. H.; Zhang, S. Q.; Liang, Y. Y.; Yang, G. W.; Yang, Y.; Yu, L. P.; Wu, Y.; Li, G. *Nature Photon.* **2009**, *3*, 649−653.
(6) Liang, Y. Y.; Xu, Z.; Xia, J. B.; Tsai, S. T.; Wu, Y.; Li, G.; Ray, C.; Yu, L. P. *Adv. Mater.* **2010**, *22*, E135−E138.
(7) Zhou, H. X.; Yang, L. Q.; Stuart, A. C.; Price, S. C.; Liu, S. B.; You, W. *Angew. Chem., Int. Ed.* **2011**, *50*, 2995−2998.
(8) Price, S., C.; Stuart, A. C.; Yang, L. Q.; Zhou, H. X.; You, W. *J. Am. Chem. Soc.* **2011**, *133*, 4625−4631.
(9) Amb, C. M.; Chen, S.; Graham, K. R.; Subbiah, J.; Small, C. E.; So, F.; Reynolds, J. R. *J. Am. Chem. Soc.* **2011**, *133*, 10062−10065.
(10) He, Z.; Zhong, C.; Huang, X.; Wong, W.-Y.; Wu, H.; Chen, L.; Su, S.; Cao, Y. *Adv. Mater.* **2011**, *23*, 4636−4643.
(11) Beaujuge, P. M.; Fréchet, J. M. J. *J. Am. Chem. Soc.* **2011**, *133*, 20009−20029.
(12) Zhang, Y.; Zou, J.; Yip, H.-L.; Chen, K.-S.; Zeigler, D. F.; Sun, Y.; Jen, A. K. Y. *Chem. Mater.* **2011**, *23*, 2289−2291.
(13) Wang, E.; Ma, Z.; Zhang, Z.; Vandewal, K.; Henriksson, P.; Inganäs, O.; Zhang, F.; Andersson, M. R. *J. Am. Chem. Soc.* **2011**, *133*, 14244−14247.
(14) Zhang, Y.; Hau, S. K.; Yip, H.-L.; Sun, Y.; Acton, O.; Jen, A. K. Y. *Chem. Mater.* **2010**, *22*, 2696−2698.
(15) Blouin, N.; Michaud, A.; Leclerc, M. *Adv. Mater.* **2007**, *19*, 2295−2300.
(16) Muhlbacher, D.; Scharber, M.; Morana, M.; Zhu, Z. G.; Waller, D.; Gaudiana, R.; Brabec, C. *Adv. Mater.* **2006**, *18*, 2884−2889.
(17) Zou, Y. P.; Najari, A.; Berrouard, P.; Beaupre, S.; Aich, B. R.; Tao, Y.; Leclerc, M. *J. Am. Chem. Soc.* **2010**, *132*, 5330−5331.
(18) Zhang, Y.; Zou, J. Y.; Yip, H. L.; Sun, Y.; Davies, J. A.; Chen, K. S.; Acton, O.; Jen, A. K. Y. *J. Mater. Chem.* **2011**, *21*, 3895−3902.
(19) Chu, T. Y.; Lu, J. P.; Beaupre, S.; Zhang, Y. G.; Pouliot, J. R.; Wakim, S.; Zhou, J. Y.; Leclerc, M.; Li, Z.; Ding, J. F.; Tao, Y. *J. Am. Chem. Soc.* **2011**, *133*, 4250−4253.
(20) Piliego, C.; Holcombe, T. W.; Douglas, J. D.; Woo, C. H.; Beaujuge, P. M.; Frechet, J. M. J. *J. Am. Chem. Soc.* **2010**, *132*, 7595.

(21) Zhang, G. B.; Fu, Y. Y.; Zhang, Q.; Xie, Z. Y. *Chem. Commun.* **2010**, *46*, 4997−4999.
(22) Su, M.-S.; Kuo, C.-Y.; Yuan, M.-C.; Jeng, U. S.; Su, C.-J.; Wei, K.-H. *Adv. Mater.* **2011**, *23*, 3315−3319.
(23) Liang, Y. Y.; Feng, D. Q.; Wu, Y.; Tsai, S. T.; Li, G.; Ray, C.; Yu, L. P. *J. Am. Chem. Soc.* **2009**, *131*, 7792−7799.
(24) Liang, Y. Y.; Wu, Y.; Feng, D. Q.; Tsai, S. T.; Son, H. J.; Li, G.; Yu, L. P. *J. Am. Chem. Soc.* **2009**, *131*, 56−57.
(25) Huo, L. J.; Hou, J. H.; Zhang, S. Q.; Chen, H. Y.; Yang, Y. *Angew. Chem. Int. Edit* **2010**, *49*, 1500−1503.
(26) van Bavel, S.; Veenstra, S.; Loos, J. *Macromol. Rapid Commun.* **2010**, *31*, 1835−1845.
(27) Yang, X.; Loos, J. *Macromolecules* **2007**, *40*, 1353−1362.
(28) Peet, J.; Kim, J. Y.; Coates, N. E.; Ma, W. L.; Moses, D.; Heeger, A. J.; Bazan, G. C. *Nat. Mater.* **2007**, *6*, 497−500.
(29) Li, G.; Shrotriya, V.; Huang, J. S.; Yao, Y.; Moriarty, T.; Emery, K.; Yang, Y. *Nat. Mater.* **2005**, *4*, 864−868.
(30) Lee, J. K.; Ma, W. L.; Brabec, C. J.; Yuen, J.; Moon, J. S.; Kim, J. Y.; Lee, K.; Bazan, G. C.; Heeger, A. J. *J. Am. Chem. Soc.* **2008**, *130*, 3619−3623.
(31) Coffin, R. C.; Peet, J.; Rogers, J.; Bazan, G. C. *Nature Chem* **2009**, *1*, 657−661.
(32) Zhu, Z.; Waller, D.; Gaudiana, R.; Morana, M.; Muhlbacher, D.; Scharber, M.; Brabec, C. *Macromolecules* **2007**, *40*, 1981−1986.
(33) Chu, T.-Y.; Lu, J.; Beaupré, S.; Zhang, Y.; Pouliot, J.-R. m.; Wakim, S.; Zhou, J.; Leclerc, M.; Li, Z.; Ding, J.; Tao, Y. *J. Am. Chem. Soc.* **2011**, *133*, 4250−4253.
(34) Krebs, F. C. *Sol. Energy Mater. Sol. Cells* **2009**, *93*, 1636−1641.
(35) Zhang, Y.; Zou, J.; Yip, H.-L.; Chen, K.-S.; Davies, J. A.; Sun, Y.; Jen, A. K. Y. *Macromolecules* **2011**, *44*, 4752−4758.
(36) Zhang, Y.; Chien, S.-C.; Chen, K.-S.; Yip, H.-L.; Sun, Y.; Davies, J. A.; Chen, F.-C.; Jen, A. K. Y. *Chem. Commun.* **2011**, *47*, 11026−11028.
(37) Qin, R. P.; Li, W. W.; Li, C. H.; Du, C.; Veit, C.; Schleiermacher, H. F.; Andersson, M.; Bo, Z. S.; Liu, Z. P.; Inganas, O.; Wuerfel, U.; Zhang, F. L. *J. Am. Chem. Soc.* **2009**, *131*, 14612−+.
(38) Liang, Y. Y.; Feng, D. Q.; Wu, Y.; Tsai, S. T.; Li, G.; Ray, C.; Yu, L. P. *J. Am. Chem. Soc.* **2009**, *131*, 7792.
(39) Liang, Y. Y.; Wu, Y.; Feng, D. Q.; Tsai, S. T.; Son, H. J.; Li, G.; Yu, L. P. *J. Am. Chem. Soc.* **2009**, *131*, 56.
(40) Scharber, M. C.; Wuhlbacher, D.; Koppe, M.; Denk, P.; Waldauf, C.; Heeger, A. J.; Brabec, C. L. *Adv. Mater.* **2006**, *18*, 789−794.
(41) Kawano, K.; Sakai, J.; Yahiro, M.; Adachi, C. *Sol. Energ. Mat. Sol. C* **2009**, *93*, 514−518.
(42) Cai, W.; Wang, M.; Zhang, J.; Wang, E.; Yang, T.; He, C.; Moon, J. S.; Wu, H.; Gong, X.; Cao, Y. *J. Phys. Chem. C* **2011**, *115*, 2314−2319.
(43) Alem, S.; Chu, T.-Y.; Tse, S. C.; Wakim, S.; Lu, J.; Movileanu, R.; Tao, Y.; Bélanger, F.; Désilets, D.; Beaupré, S.; Leclerc, M.; Rodman, S.; Waller, D.; Gaudiana, R. *Org. Electron.* **2011**, *12*, 1788−1793.
(44) Park, C.-D.; Fleetham, T. A.; Li, J.; Vogt, B. D. *Org. Electron.* **2011**, *12*, 1465−1470.
(45) Hoth, C. N.; Steim, R.; Schilinsky, P.; Choulis, S. A.; Tedde, S. F.; Hayden, O.; Brabec, C. J. *Org. Electron.* **2009**, *10*, 587−593.
(46) Zhao, J.; Swinnen, A.; Van Assche, G.; Manca, J.; Vanderzande, D.; Mele, B. V. *J. Phys. Chem. B* **2009**, *113*, 1587−1591.
(47) He, C.; Zhong, C.; Wu, H.; Yang, R.; Yang, W.; Huang, F.; Bazan, G. C.; Cao, Y. *J. Mater. Chem.* **2010**, *20*, 2617−2622.
(48) Seo, J. H.; Gutacker, A.; Sun, Y.; Wu, H.; Huang, F.; Cao, Y.; Scherf, U.; Heeger, A. J.; Bazan, G. C. *J. Am. Chem. Soc.* **2011**, *133*, 8416−8419.
(49) He, Z.; Zhang, C.; Xu, X.; Zhang, L.; Huang, L.; Chen, J.; Wu, H.; Cao, Y. *Adv. Mater.* **2011**, *23*, 3086−3089.
(50) Zou, J.; Yip, H.-L.; Zhang, Y.; Gao, Y.; Chien, S.-C.; O'Malley, K.; Chueh, C.-C.; Chen, H.; Jen, A. K. Y. *Adv. Funct. Mater.* **2012**, DOI: 10.1002/adfm.20110293.
(51) Yip, H.-L.; Jen, A. K. Y. *Energ. Environ. Sci.* **2012**, *5*, 5994−6011.
(52) Li, C.-Z.; Yip, H.-L.; Jen, A. K. Y. *J. Mater. Chem.* **2012**, *22*, 4161−4177.
(53) Ma, H.; Yip, H.-L.; Huang, F.; Jen, A. K. Y. *Adv. Funct. Mater.* **2010**, *20*, 1371−1388.
(54) O'Malley, K. M.; Li, C.-Z.; Yip, H.-L.; Jen, A. K. Y. *Adv. Energy Mater.* **2012**, *2*, 82−86.
(55) Li, C. Z.; Chueh, C. C.; Yip, H. L.; O'Malley, K. M.; Chen, W. C.; Jen, A. K. Y. *J. Mater. Chem.* **2012**, *22*, 8754−8578.